nature geoscience

SUPPLEMENTARY INFORMATION

DOI: 10.1038/NGEO1985

Two-phase change in CO_2, Antarctic temperature and global climate during Termination II

1- Phase relationship between the CO_2 concentration and Antarctic temperature change during Termination II

Because past variations in atmospheric CO_2 concentrations are measured in the gas phase while the classical temperature proxy, δD, is measured in the ice phase of ice cores, evaluating their phase relationships requires quantification of the depth difference between a synchronous event recorded in the ice and gas phases (Δdepth) or the age difference between gas and ice at the same depth (Δage). This depth or age difference has commonly been estimated using firnification models[S1, S2, S3]. In low accumulation rate sites of central East Antarctica, independent Δdepth estimates have revealed that these models appear to systematically overestimate Δdepth under glacial conditions at these sites[S4, S5], challenging their use for estimating the CO_2-Antarctic temperature timing under glacial conditions.

The isotopic composition of nitrogen ($\delta^{15}N$ of N_2, hereafter $\delta^{15}N$) or argon ($\delta^{40}Ar$ of Ar) in air trapped in ice cores, can be used to assess past changes in Δdepth. Indeed, assuming that the firn structure remains roughly the same over glacial-interglacial changes (constant depth of convective zone, constant average firn density and constant vertical temperature gradient), $\delta^{15}N$ changes enable to estimate changes in lock-in depth (LID, where air no longer diffuses in the firn) during Termination I[S4]. Alternatively a record of $\delta^{40}Ar$ during Termination III was interpreted as an indicator of surface temperature and/or accumulation rate changes in the gas phase[S6]. The strong influence of accumulation rate on $\delta^{15}N$ evolution over deglaciation has been recently confirmed on a compilation of $\delta^{15}N$ measurements at different Antarctic sites[S5]. Over Termination III, Vostok temperature and/or accumulation rate changes were shown to lead changes in atmospheric CO_2 concentration by 800 ± 200 years on average.

Figure S1 displays the complete high-resolution $\delta^{15}N$ profile measured at the Laboratoire des Sciences du Climat et de l'Environnement (LSCE) over Termination II and the last interglacial period, consisting of 20 duplicated depth levels already published[S7] and 130 new depth levels measured in 2010 using a melt-refreeze method for air extraction and dual inlet mass spectrometry for measurements[S8] of $\delta^{15}N$ of N_2. The resulting uncertainty on $\delta^{15}N$

measurement over this series of measurements is of 5 ppm (1 σ). The average depth resolution is 2.75 m corresponding to an age resolution of 200 years over Termination II. We therefore reach a temporal resolution similar to that of available CO_2 measurements[S9] over Termination II and completed in this study by 12 additional measurements at the start of Termination II on the same ice core (Figure 1).

Using the EDC3 gas and ice timescales[S10,S11], δD and $\delta^{15}N$ are highly correlated (R^2 of 0.85**,** n= 150) with a lag of $\delta^{15}N$ with respect to δD by ~3 ka over the optimum of the last interglacial period. Polar precipitation δD is an integrated tracer of the water cycle, which is not only affected by changes in condensation temperature but also by changes in evaporation conditions (isotopic composition, surface temperature and humidity at evaporative sources). After accounting for source conditions using the second-order parameter deuterium excess, Stenni et al.[S12] have estimated changes in EDC site temperature (T_{site}). The comparison between T_{site} and $\delta^{15}N$ shows a slightly stronger correlation compared to the one obtained with δD (R^2=0.89, n=150). During the glacial inception, around 115 kyrs BP, $\delta^{15}N$ and T_{site} synchronously decrease (Figure 2). This comparison confirms the inference of Stenni et al.[S12] that δD is affected by warm source conditions at the glacial inception, which enhance isotopic depletion.

The good correlation between $\delta^{15}N$ and both δD and T_{site} on their EDC3 timescales supports a previous conclusion[S6,S7] that glacial-interglacial variations of $\delta^{15}N$ are driven by changes in surface temperature and/or accumulation rate. Accumulation rate changes in ice cores are assumed to be driven by variations of surface temperature through an exponential law[S13] and this general relationship between accumulation rate and temperature is in general agreement with layer counting measurements in Greenland ice cores[S14]. As a consequence, both accumulation rate and temperature variations are expected to be in phase with δD variations in ice cores. Recently, changes in dust content have been suggested to be an additional driver of snow metamorphism and firn depth[S15]. A recent compilation of coastal to central Antarctic $\delta^{15}N$ records spanning the last deglaciation did however not exhibit any obvious relationship between dust concentration and $\delta^{15}N$, while the correlations between $\delta^{15}N$ and δD variations were shown to be robust with an important influence of changes in accumulation rate on $\delta^{15}N$ variations[S5]. During Termination II, the onset of EDC dust concentration decrease coincides with the start of δD increase[S16, S17], hence at much shallower depth (30 m) than the start of the $\delta^{15}N$ increase which can therefore not be explained by the increase in dust concentration near the firn pore close-off. Moreover, the dust concentration

reaches an interglacial level quickly, about 2.5 ka before δD[S16, S17]. If dust concentration was the primary driver of $\delta^{15}N$, a decoupling between $\delta^{15}N$ and δD should be recorded during the intervals of large dust variations but this is not observed. Still, we cannot rule out a lag between changes in surface temperature / accumulation rate and $\delta^{15}N$ at firn close-off. However, we can safely consider that $\delta^{15}N$ did not change before and more rapidly than temperature / accumulation rate at the surface.

With these limitations in the interpretation of $\delta^{15}N$ in mind, we now compare $\delta^{15}N$ evolution over Termination II with the EDC record of CO_2 on the same depth scale (Table 1, Figure 3). Comparing the two evolutions is not easy because the rate of δD, $\delta^{15}N$ and CO_2 increases are not constant over Termination II. This is especially true for the end of Termination II where the rate of increase in $\delta^{15}N$ slows at ~1750 m (when interglacial $\delta^{15}N$ values are reached). $\delta^{15}N$ values then continue to increase slowly until the optimum of MIS 5.5 is reached at ~1716 m. In contrast CO_2 reaches a plateau between 1741 m and 1724 m before the overshoot occurring in phase with the $\delta^{15}N$ maximum at the MIS 5.5 optimum. Despite these slight differences in behaviors at the end of Termination II, we have chosen to use a determination based on the Rampfit software[S18] to compare objectively the onsets and mid-slopes of the main increases in levels of CO_2, $\delta^{15}N$, and δD (Table 1). We used depth windows of 1680 – 1840 m for the gas phase and 1620-1780 m for the ice phase (or the equivalent time windows).

While the onsets of $\delta^{15}N$ and CO_2 cannot be distinguished within the ~2 m uncertainty, we see a clear lead of $\delta^{15}N$ over CO_2 at the mid-slope (10.2 ± 3.6 m) of the main increasing phase of Termination II. This lead is not modified if we remove the CO_2 inflexion point at 1741.3 m and the associated error bar is only increased by 0.17 m. The rate of increase in $\delta^{15}N$ is thus greater than for CO_2 resulting in $\delta^{15}N$ achieving its mid-points ahead of CO_2. This result is robust regardless of differences in behavior of these two parameters during the last interglacial, as discussed above. Over the last part of the Termination II, quantifying the visible lead of $\delta^{15}N$ over CO_2 is not easy since both signals show a different dynamic with a slow and rather constant increase for $\delta^{15}N$ versus a plateau followed by an overshoot for CO_2.

Assuming that the firn structure did not change over time (no convective zone)[S19], $\delta^{15}N$ can be used as an indicator of LID. We therefore apply the method proposed by Bender et al.[S20] and Parrenin et al.[S4] to Termination II at EDC. The depth difference, Δdepth, between

concomitant change in gas and ice phases is calculated[S4] from (i) the thinning value at the depth of Termination II and (ii) the lock-in depth inferred from $\delta^{15}N$ and the barometric equation. The main limitation of this approach lies in the ~10 % uncertainty in the thinning function at 1700 m depth, which leads to a 3.5 m uncertainty on the Δdepth calculation. While this uncertainty prevents us from firm conclusions on the mid-slope lead or lag of CO_2 vs temperature, we note that the shape of the δD increase, when shifted by Δdepth, is very close to the $\delta^{15}N$ increase (difference of 2 m) which supports our use of $\delta^{15}N$ as a proxy for δD in the gas phase. The same exercise has been done over Termination III at Vostok comparing the results obtained by Caillon et al.[S6] and our Δdepth approach using in this case a convective zone of 13 m as for present-day Vostok conditions[S20]. Again the two approaches give similar results despite large uncertainties in the Δdepth approach (Figure S4).

Finally, our most robust finding is that the initial increase in $\delta^{15}N$ and CO_2 occur synchronously, within uncertainty, and that the mid-slope of $\delta^{15}N$ increase (which cannot precede changes in temperature and accumulation over Termination II as discussed above through its link with δD or T_{site} and timing of dust increase) occurs prior to the mid-slope of CO_2 increase. At mid-slopes, the increase in $\delta^{15}N$ leads by 900 ± 325 years those of CO_2. We know from modeling studies that Antarctic temperature is not a linear function of CO_2 concentration[S21]. This is due to the following logarithmic relationship[S22] between radiative forcing (RF) and the atmospheric concentration of CO_2.

$$RF\ (W.m^{-2}) = 5.35\ \ln(CO_2/CO_{2,0}) \text{ with } CO_{2,0} = 278 \text{ ppm.} \quad \text{(Equation 1)}$$

We have thus repeated our ramp analysis using the radiative forcing of CO_2 (Table S1) deduced from Equation (1). In this case, $\delta^{15}N$ still leads CO_2 radiative change by 675 ± 350 years at mid-slope.

2- High resolution measurements of $\delta^{18}O_{atm}$ over Termination I and Termination II.

$\delta^{18}O$ of O_2 is measured on the same samples than $\delta^{15}N$ of N_2. For measurements performed at LSCE, the same melt-refreeze method is used[S8] and the same dual inlet mass spectrometer run measures $\delta^{15}N$ of N_2 and $\delta^{18}O$ of O_2 using a Thermo Delta V equipped with masses 28, 29, 30, 32, 33, 34 and 44. For measurements performed at Princeton, the headspace equilibration method inspired from Emerson et al.[S23] and improved by Dreyfus et al.[S7] has

been applied. Simultaneous measurements of $\delta^{15}N$[S7] and $\delta^{18}O$ were achieved using a Delta Plus XP mass spectrometer. For both sets of measurements, corrections for CO^+ influence on mass 28 and for influences of the $\delta O_2/N_2$ on $\delta^{15}N$ and $\delta^{18}O$ values are done[S8,S24].
A gas loss effect has been shown to influence measurements of both $\delta^{18}O$ of O_2 and $\delta O_2/N_2$ in air trapped in ice core with a constant slope[S25,S26,S27,S28] of 0.01‰/‰ between the changes in $\delta O_2/N_2$] so that the corrected $\delta^{18}O$ of O_2 is calculated as[S29]:

$$\delta^{18}O_{corr} = \delta^{18}O_{measured} + (\delta O_2/N_2 + 10) \times 0.01$$

To separate the firn and atmospheric fractionation processes, the influence of gravitational fractionation in the firn is removed from corrected $\delta^{18}O$ of O_2 using the $\delta^{15}N$ measurements so that:

$$\delta^{18}O_{atm} = \delta^{18}O_{corr} - 2\,\delta^{15}N$$

The final uncertainty attached to $\delta^{18}O_{atm}$ values at each level is of 0.025 ‰ (1 σ) for the series of data from Termination II and Termination I presented here.

3- Measurements of CO_2 concentration

The CO_2 data plotted on Figure 2 include 2 sets of measurements. The first set was obtained from the published data by Lourantou et al.[S9] while the second one has been obtained for this study. The same extraction method has been used in both cases, i.e. 40 – 50g of ice are placed under vacuum and crushed in a steel ball mill.
In the case of the Lourantou et al.[S9] set, CO_2 and its carbon isotopic ratio measurements are coupled. The extracted gas is expanded in a 10 cm^3 sample loop. From there, an ultra pure helium stream flushes the gas through a glass trap where CO_2 is frozen out at −196 °C. The trapped CO_2 is then transferred into a low flow rate helium stream, to be cryofocused on a small volume glass capillary tubing also at −196 °C. The subsequent warming of the capillary allows the gas transfer through a gas chromatograph to separate the CO_2 from residual impurities such as N_2O and its introduction in the isotope ratio mass spectrometer IRMS (Finnigan MAT 252). The CO_2 mixing ratio in the ice samples is deduced from a linear regression between standard gas injections (CO_2 = 260.26 ± 0.2 ppmv in dry air) at different

pressures and the corresponding CO_2 peak amplitude measured by the IRMS. Each sample or external standard introduction in the IRMS is bracketed with injections of a pure CO_2 standard reference gas (internal standard, ATMO MESSER, $\delta^{13}C$ of -6.5 ± 0.1‰ versus VPDB). Each result of ice core gas sample consists of the mean of three consecutive measurements of the same sample gas stored in the extraction container and expanded three times. For this analytical series on Termination II EDC samples, the pooled standard deviation associated with the average value of three replicate measurements of the same extracted gas amounts to 1.9 ppmv for CO_2.

In the case of the new set of measurements (this work), the extracted gas is expanded in a 1 cm^3 sample loop and flushes with an ultra pure helium stream through inox tubing line. A Gas Chromatograph (GC) Varian 3300 separates the CO_2, reduces it to CH_4 through a methanizer, and with a Flame Ionised Detector produces an electrical signal proportional to the concentration. The CO_2 mixing ratio is deduced using the same protocol as Lourantou et al. We use a linear regression between standard gas injections ($CO_2 = 232.6 \pm 0.2$ ppmv) at different pressures and the corresponding CO_2 peak amplitude measured by the GC. Each ice core gas sample result is calculated as the mean of minimum 4 replicate measurements of the same sample gas stored in the extraction cell. The standard deviation associated with the average value of replicate measurements amounts to 1.3 ppmv.

We note the good agreement between the 2 sets of measurements, which have been obtained with 2 different analytical procedures.

References:

S1 Monnin et al. Atmospheric CO_2 concentrations over the last glacial termination. *Science* **291,** 112-114 (2001)

S2 Fischer, H., Wahlen, M., Smith, J., Mastroianni, D. & Deck, B., Ice Core Records of Atmospheric CO2 Around the Last Three Glacial Terminations. *Science* **283,** 1712-1714 (1999)

S3 Pedro, J. B., Rasmussen, S. O. & van Ommen, T. D. Tightened constraints on the time-lag between Antarctic temperature and CO_2 during the last deglaciation. *Clim. Past* **8,** 1213-1221 (2012)

S4 Parrenin, F. et al. On the gas-ice depth difference (Δdepth) at EPICA Dome C. *Clim. Past* **8,** 1239-1255 (2012).

S5 Capron, E. et al. Glacial-interglacial dynamics of Antarctic firn columns: comparison between simulations and ice core air-δ15N measurements. *Clim. Past Discuss* **8,** 6051-6091 (2012)

S6 Caillon, N. et al. Timing of atmospheric CO_2 and Antarctic temperature changes across Termination III. *Science* **299,** 1728-1731 (2003)

S7 Dreyfus G.B. et al. Firn processes and d15 N: potential for a gas-phase climate proxy. *Quaternary Science Reviews* **29,** 222-234 (2010)

S8 Landais A., Caillon, N., Severinghaus, J.P., Jouzel, J., & Masson-Delmotte,V. Analyses isotopiques à haute précision de l'air piégé dans les glaces polaires pour la quantification des variations rapides de température : méthode et limites. *Notes des Activités Instrumentales de l'IPSL* **39,** 1-15 (2003)

S9 Lourantou, A., Chappellaz, J., Barnola, J.-M., Masson-Delmotte, V. & Raynaud, D. Changes in atmospheric CO_2 and its carbon isotopic ratio during the penultimate deglaciation. *Quaternary Science Reviews.* **29,** 1983-1992 (2010)

S10 Parrenin, F. et al. The EDC3 agescale for the EPICA Dome C ice core. *Clim. Past* **3,** 485-497 (2007).

S11 Loulergue, L. et al. New constraints on the gas age-ice age difference along the EPICA ice cores, 0–50 kyr. *Clim. Past* **3,** 527-540 (2007)

S12 Stenni, B. et al. The deuterium excess records of EPICA Dome C and Dronning Maud Land ice cores (East Antarctica). *Quaternary Science Reviews* **29,** 146-159 (2010)

S13 Lorius, C., Merlivat, L. & Hagemann, R. Variation in mean deuterium content of precipitations in Antarctica. *Journal of Geophysical Research* **74,** 7027-7037 (1969)

S14 Rasmussen, S.O. et al. Synchronization of the NGRIP, GRIP, and GISP2 ice core across MIS 2 and palaeoclimatic implications. *Quaternary Science Reviews* **27,** 18-28 (2008)

S15 Hörhold, M. W. et al. On the impact of impurities on the densification of polar firn. *Earth and Planetary Science Letters* ***325*****,** 93-99 (2012)

S16 Lambert F. et al. Dust-climate couplings over the past 800,000 years from the EPICA Dome C ice core. *Nature* **452,** 616-619 (2008).

S17 Röthlisberger, R. et al. The Southern Hemisphere at glacial terminations: insights from the Dome C ice core. *Climate of the Past* **4,** 345-356 (2008)

S18 Mudelsee, M. Ramp function regression: a tool for quantifying climate transitions. *Comput. Geosci.* **26,** 293–307 (2000)

S19 Landais, A. et al. Firn-air d15N in modern polar sites and glacial-interglacial ice: a model-data mismatch during glacial periods in Antarctica? *Quaternary Science Reviews* **25,** 49-62 (2006)

S20 Bender, M. L. et al. Gas age-ice age differences and the chronology of the Vostok ice core, 0-100 ka, *Journal of Geophysical Research - Atmospheres* **111,** D21115 (2006)

S21 Ganopolski, A. & Roche, D. On the nature of lead-lag relationships during glacial-interglacial climate transitions, *Quaternary Science Reviews* **37/38,** 3361-3378 (2009)

S22 Joos, F. Radiative forcing and the ice core greenhouse gas record. *PAGES Newsletters* **13/3**, 11-13 (2005)

S23 Emerson, S., Quay, P., Stump, C., Wilbur, D. & Schudlich, R. Chemical tracers of productivity and respiration in the subtropical Pacific Ocean. *J. Geophys. Res.* **100,** 15873–15887 (1995).

S24 Severinghaus, J. P., Grachev A. & Battle, M., Thermal fractionation of air in polar firn by seasonal temperature gradients. *Geochemistry, Geophysics, Geosystems*. **2,** 2000GC000146 (2001)

S25 Landais A. et al. A tentative reconstruction of the last interglacial and glacial inception in Greenland based on new gas measurements in the Greenland Ice Core Project (GRIP) ice core. *J. Geophys. Res.* **108,** 4563 (2003)

S26 Dreyfus, G. B. et al. Anomalous flow below 2700m in the EPICA Dome C ice core detected using 18O of atmospheric oxygen measurements. *Clim. Past* **3,** 341–353 (2007)

S27 Suwa, M. & Bender, M.L. O_2/N_2 ratios of occluded air in the GISP2 ice core. *J. Geophys. Res.* **113,** D11119 (2008).

S28 Severinghaus, J.P., Beaudette, R.A., Headly, M., Taylor, K. & Brook, E. J. Oxygen-18 of O_2 Records the Impact of Abrupt Climate Change on the Terrestrial Biosphere. *Science* **324,** 1431-1434 (2009)

S29 Landais, A. et al. What drives the orbital and millennial variations of $\delta^{18}O_{atm}$? *Quaternary Science Reviews* **292,** 235-246 (2010)

S30 Loulergue, L. et al. Orbital and millennial-scale features of atmospheric CH_4 over the past 800,000 years. *Nature* **453,** 383-386 (2008)

Table S1 : Results from a Rampfit analysis to quantify the start, mid slope and end of Termination II increases in δD, accumulation rate (in the ice depth), $\delta^{15}N$ and δD shifted by Δdepth, atmospheric CO_2 concentration and CO_2 radiative forcing (in the gas depth). All depths and the associated uncertainties are reported in meters of ice.

units: meters	depth_bot	uncertainty	depth_top	uncertainty	depth_mid	uncertainty
δD	1771.5	4.1	1712.7	3.1	1742.8	1.8
accumulation rate	1766	5.6	1714.9	5.9	1740.5	3.1
$\delta^{15}N$	1793	2.9	1749	2.1	1771	1.8
δD shifted by Δdepth	1791.4	4.4	1747.3	3	1769.4	1.9
CO_2	1796.8	2.7	1724.8	3.6	1760.8	1.8
CO_2 forcing	1801.8	3.1	1724.8	3.8	1763.3	1.9

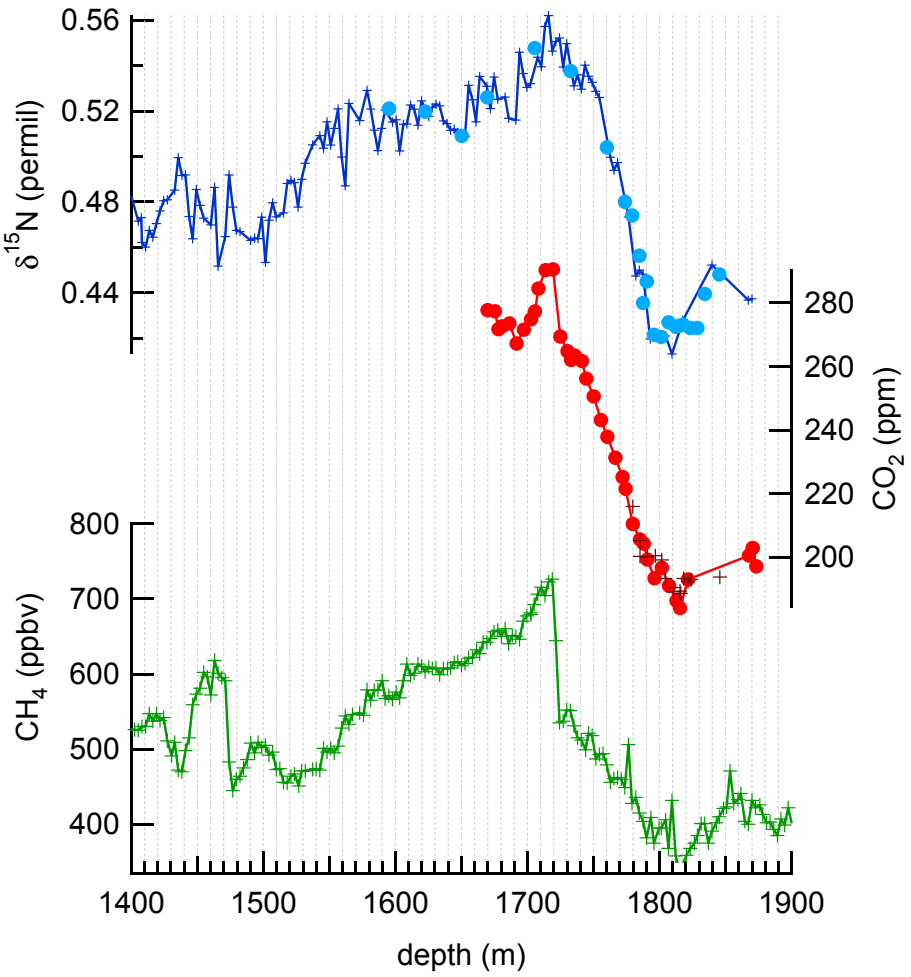

Figure S1 :

Top: new $\delta^{15}N$ data (blue crosses) and previously published $\delta^{15}N$ data (blue circles[S7]) from the EDC ice core. The analytical accuracy of replicate measurements is 6 per meg.

Middle: new CO_2 data (brown crosses) and previously published CO_2 data (red circles[S9]) from the EDC ice core.

Bottom: Atmospheric CH_4 concentrations (ppbv) from EDC[S30]

.

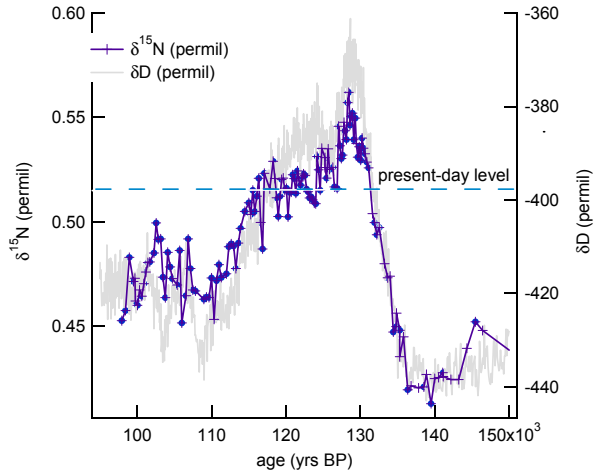

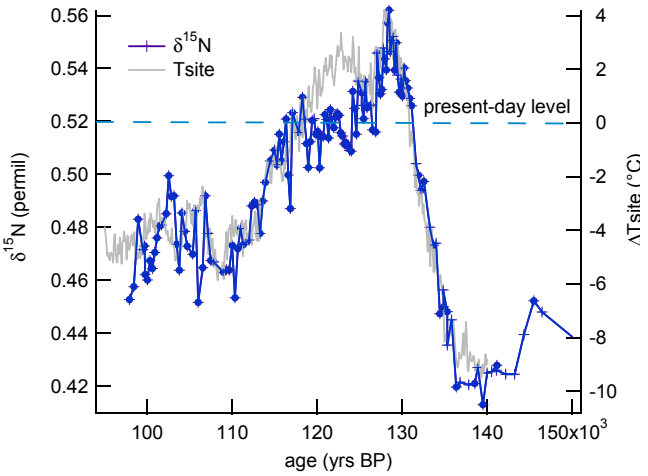

Figure S2a (left):

Comparison of $\delta^{15}N$ and δD records on the EDC3 gas and ice timescales respectively. The vertical scales have been adjusted around the present-day levels of $\delta^{15}N$ and δD.

Figure S2b (right):

Comparison of the $\delta^{15}N$ and T_{site} records on the EDC3 timescale. The vertical scales have been adjusted around the present-day levels of $\delta^{15}N$ and T_{site}.

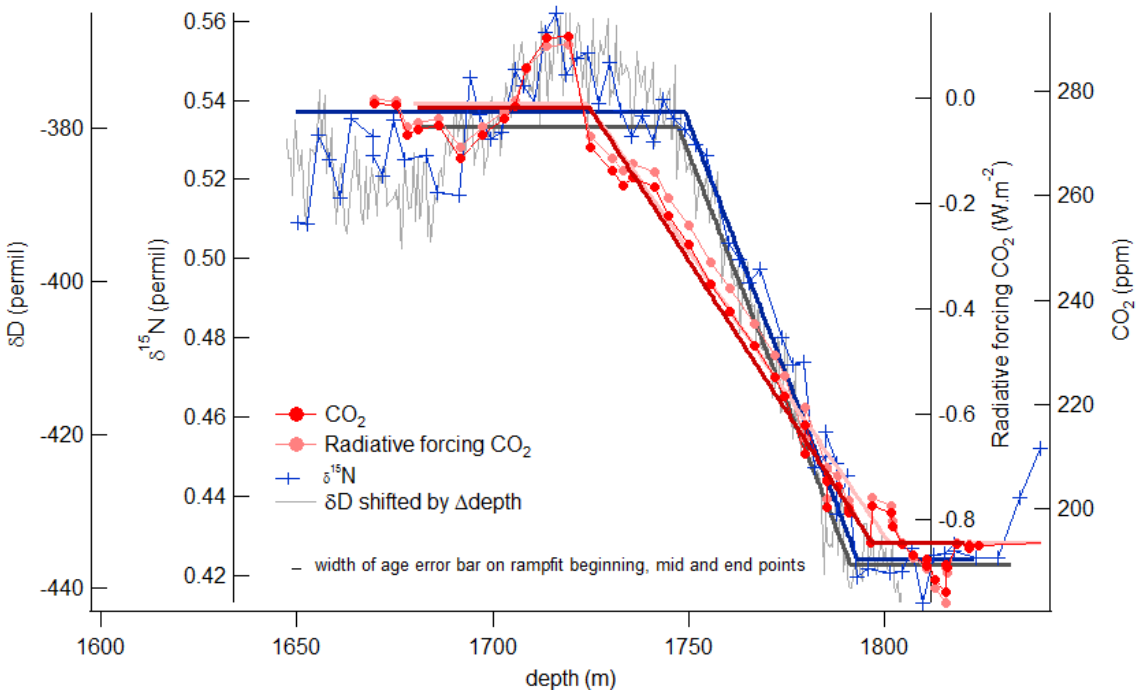

Figure S3:

Evolutions of $\delta^{15}N$ (blue), CO_2 (red), radiative forcing of CO_2 (pink) and δD shifted by Δdepth (grey) following the approach by Parrenin et al.[S4] over Termination 2. Linear segments obtained using the Rampfit software[S18] are represented as solid lines of the same color of each record.

Note that the ramp is not modified when removing the CO_2 inflexion point at 1741.3 m depth.

The radiative forcing of CO_2 is calculated following Equation (1)

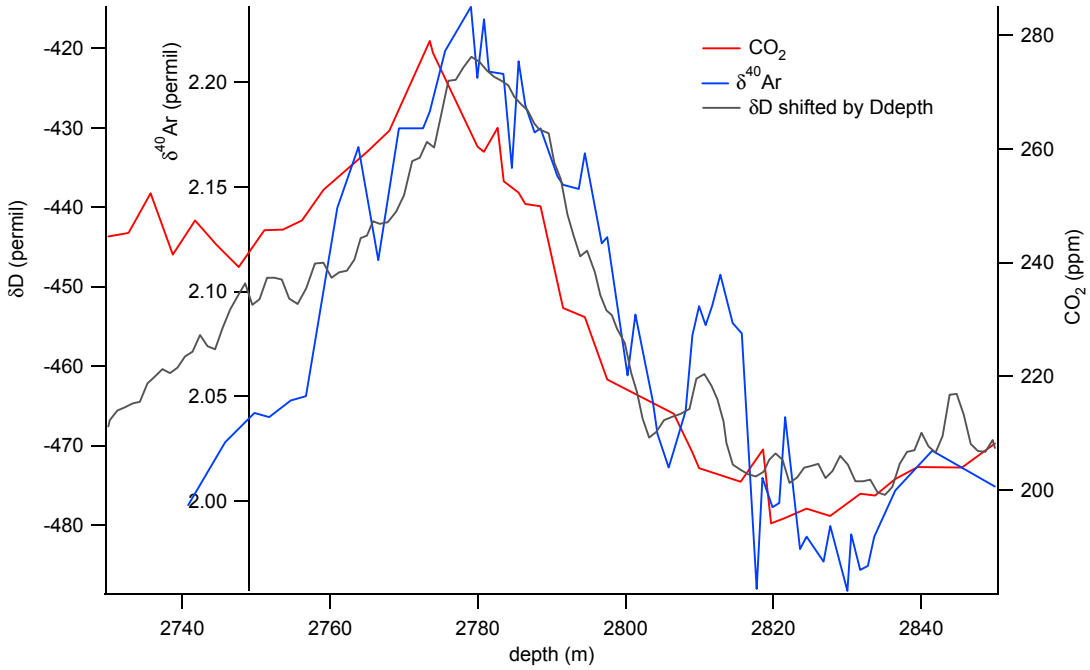

Figure S4:

Evolutions of $\delta^{40}Ar$ (blue), CO_2 (red) and δD shifted by Δdepth (grey) following the approach by Parrenin et al.[S4] over Termination II.